WORLD SCIENTIFIC SERIES ON ASIA-PACIFIC WEATHER AND CLIMATE

Vol. 6

Climate Change

Multidecadal and Beyond

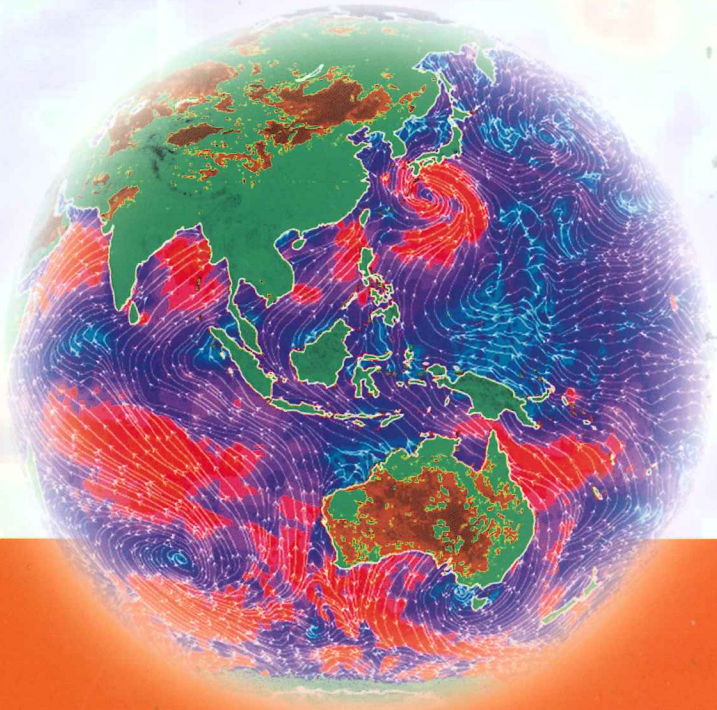

edited by

Chih-Pei Chang • Michael Ghil

Mojib Latif • John M. Wallace

World Scientific

Chapter 22

The South-Flood North-Drought Pattern Over Eastern China and the Drying of the Gangetic Plain

Sumant Nigam, Yongjing Zhao and Alfredo Ruiz-Barradas
Department of Atmospheric Science,
University of Maryland, College Park, MD 20742, USA

Tianjun Zhou
LASG, Institute of Atmospheric Physics,
Chinese Academy of Sciences, Beijing, 100029, China
nigam@umd.edu

The Indo-Gangetic Plain and the lowlands/plains eastward of the Tibetan Plateau exhibit substantial — at times, precarious — trends in summer precipitation since the mid-20th century. These include the declining rainfall over the Gangetic Plain, and a dipole trend pattern over eastern China that is referred as the South-Flood North-Drought (SFND) pattern. The trends have been attributed to increased aerosol and dust loadings, significant land-use land-cover change, and increased greenhouse gas emissions, among others. Interestingly, multidecadal natural variability is not a commonly cited cause. The presence of oppositely-signed trends in the first-half of the 20th century in some of the same regions prompted this reassessment of the role of multidecadal SST variability in generation of rainfall trends over monsoon Asia.

Analysis of the century-long precipitation and SST records suggests that the post-1950 decline in rainfall over the northwestern-central Gangetic Plain and northeastern China is linked with North Pacific decadal SST variability. The rainfall decline over the Himalayan foothills and northeastern Gangetic Plain, and increasing rainfall over the lower Yangtze River basin (the southern SFND center), on the other hand, are found linked with SST Secular Trend (or secular variability) in this analysis.

The SST anomalies associated with North Pacific decadal variability extend well beyond the midlatitude Pacific — into the tropical Indian and Pacific basins where oppositely signed SST anomalies are present. It is hypothesized that the tropical Indian Ocean SST anomalies modulate the meridional ocean-continent thermal contrast, and thus the large-scale distribution of monsoon rainfall over the Asian continent. The findings need corroboration from additional analyses of the observed circulation and thermodynamics fields, and the hypothesis support from controlled climate model experiments.

1. Introduction

The Indo-Gangetic Plain extending from eastern Pakistan to the Bay of Bengal and the lowlands and plains eastward of the Tibetan Plateau are home to two billion people, and the agricultural heartland of Asia. Rapid population and economic growth have led to significant land-use land-cover change, heightened demand for fresh water and energy, degraded environment from dust and aerosol loadings, and increased greenhouse gas emissions.

Climate Change: Multidecadal and Beyond
edited by Chih-Pei Chang et al.

Regional hydroclimate (precipitation, surface air temperature, soil moisture, subsurface water) exhibits substantial — at times, precarious — trends across the second half of the 20th Century. The post-1950 summer rainfall trend (Fig. 1) is impressive over the Ganges River basin as it represents a decline of 2 mm/day over a 60-year period against climatology of 8–10 mm/day (not shown). A coherent meridional dipole over eastern China, with significant drying in the middle and lower reaches of the Yellow River (where climatological rainfall is less than 4 mm/day) and increasing rainfall across and to the south of the Yangtze River is also evident. The anomalous rainfall pattern is often referred as the South-Flood North-Drought (SFND) pattern (Yu and Zhou, 2007; Zhou *et al.*, 2009a).

The SFND pattern and the drying of the Gangetic Plain are robust trends given their unambiguous presence in independent analyses of observed precipitation. Figure 1 shows the trends in CRU TS3.1 (0.5°, Mitchell and Jones, 2005), WCRP GPCC (0.5°, Schneider *et al.*, 2011), University of Delaware (0.5°, Willmott and Matsuura, 1995), Chinese Meteorological Administration (station data), and the Aphrodite (0.5°, Yatagai *et al.*, 2009) analyses. The Gangetic Plain trend is more variable of the two, and likely overestimated in the CRU analysis. The CRU data is nonetheless analyzed in view of our interest in the surface air temperature trends as well.

The SFND pattern is manifest also in the Yellow and Yangtze River discharge and other hydroclimate variables despite anthropogenic impacts (*e.g.*, water withdrawal). The annual river discharge at downstream stations in eastern China is shown in Fig. 2, while recent trends in the surface water equivalent (SWE) from the GRACE satellite gravity solutions are shown in Fig. 3; both supporting the SFND rainfall trend pattern. The GRACE solutions also capture the declining water stores in the Gangetic Plain.

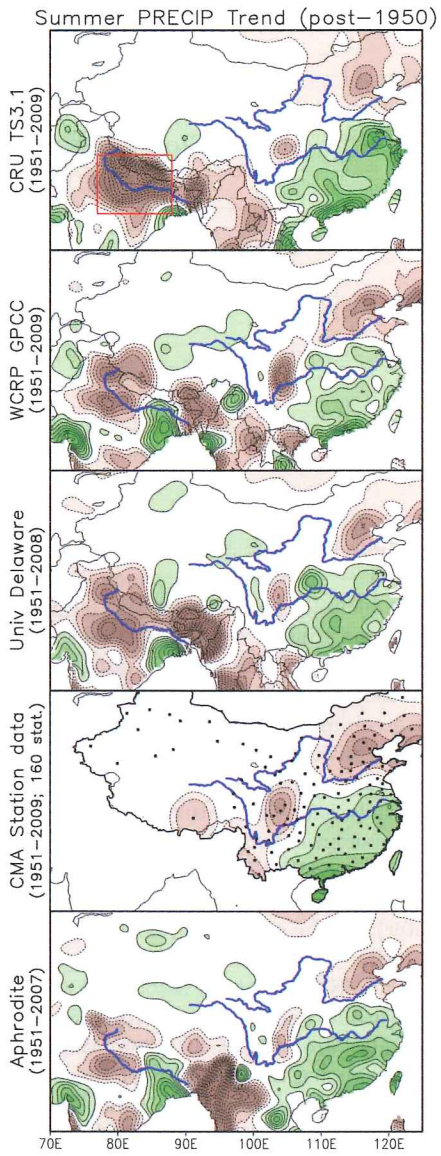

Fig. 1. The linear trend in summer (JJA) rainfall in the post-1950 period in the CRU TS 3.1, WCRP GPCC, University of Delaware, Chinese Meteorological Administration (CMA), and the Aphrodite analysis of observed precipitation. The trend over the recent 60-year period is shown; the exact period is stated in the left labels. The trend is plotted at 0.5 mm/day/century interval, with deficit/surplus shown in brown/green, and the zero-contour omitted. The Ganges River in the Indian subcontinent and the Yangtze and Yellow rivers in China are marked in blue for regional reference. The South-Flood North-Drought (SFND) pattern over eastern China, and the drying of the Gangetic Plain is manifest in various analyses.

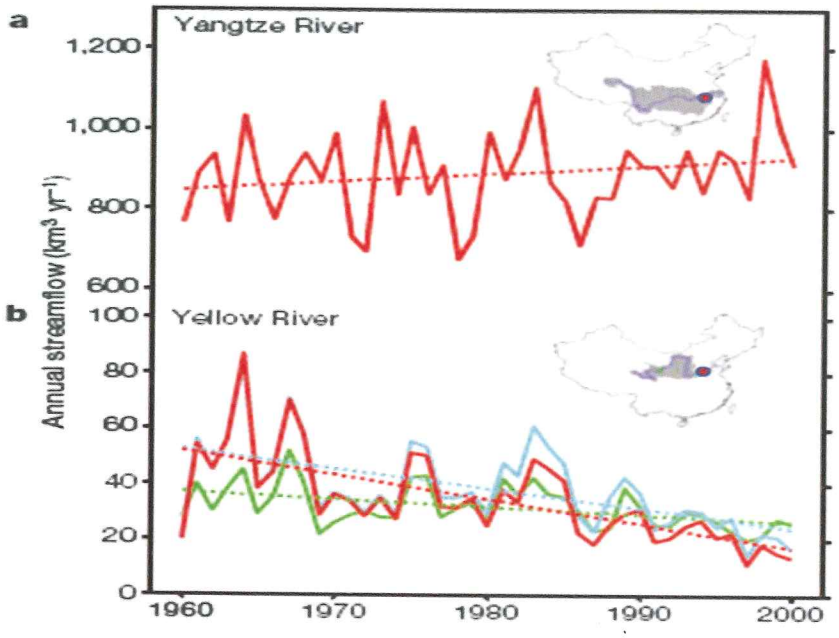

Fig. 2. Interannual variations in annual runoff during 1960–2000 at the Datong station in the lower Yangtze River (top), and Gaocun station in the lower Yellow River (bottom), both in red; from Piao *et al.* (2010); the stations are marked by solid dots. The green and blue curves in the lower panel are for the upstream stations on the Yellow river.

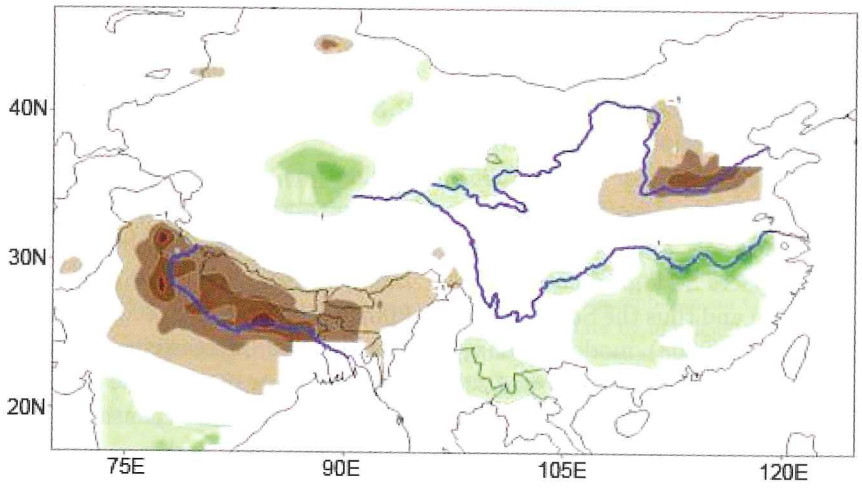

Fig. 3. Linear trend in the summer terrestrial water equivalent thickness during 2003–2010 from the GRACE satellite gravity solutions. Brown (greens) denote depletion (accumulation) of ground water; contour interval is 1 cm/year and the zero-contour omitted. Note the declining trend over the Gangetic Plain and the South-Flood North-Drought pattern over eastern China.

The summer circulation over the Asian continent and the surrounding oceans also exhibits significant trends during the same period, *e.g.*, westward expansion of the Western Pacific Subtropical High (WPSH) since the 1970s. The expansion was attributed to the warming of the Indian Ocean and the Western Pacific, from modeling of the atmospheric response of specified SST anomalies (Zhou *et al.*, 2009b). This modeling analysis (with idealized SST anomalies) was however unable to generate the SFND rainfall pattern or the drying of the Gangetic Plain in a convincing manner.

Is the steep decline in summer monsoon rainfall over the Gangetic Plain and northeastern China indicative of accelerated anthropogenic effects (from human imprints on greenhouse gas emissions, aerosol/dust loadings, land-use land-cover degradation, and groundwater irrigation), multidecadal ocean variability, or both?

2. Possible Mechanisms

2.1. *Aerosols*

Increasing aerosol loadings over South Asia since the 1950s have been advanced as one cause of the declining summer precipitation trend over the Gangetic Plain. Ramanathan *et al.* (2005) have emphasized the short wave (SW) absorption of black carbon aerosols, and related surface 'dimming', which impacts SST gradients in the northern Indian Ocean and thus the South Asian monsoon; Meehl *et al.* (2008) modeling analysis corroborates this assessment. The aerosol SW absorption also leads to heating of the lower-to-mid troposphere, altering static stability, tropospheric temperature gradients, and thus the monsoon (Menon *et al.*, 2002; Lau *et al.*, 2006). Bollasina *et al.* (2011), on the other hand, argue for the importance of aerosol SW reflection and the resulting cooling of the Asian continent to be the cause of declining summer rainfall over South Asia in the post-1950 period.

The aerosols generate declining summer rainfall also over East Asia in the Bollasina *et al.* analysis, in contrast with the observed increasing trend in regional rainfall (the South-Flood part of the SFND rainfall trend pattern). Atmospheric model simulations produced with historical forcing (prescribed SSTs, greenhouse gases, and direct aerosol effects) have also been unsuccessful in generating the SFND pattern (Li *et al.*, 2010).

2.2. *Land-use land-cover change*

Rainfall decline over the Gangetic Plain has also been attributed to increasing desertification over northwestern India. Bollasina and Nigam (2011) found an expanded Thar Desert linked with reduced summer monsoon rainfall over eastern India in a modeling analysis of regional hydroclimate change over the Indian subcontinent. The low-level anticyclone forced by increased desert subsidence generates northwesterly flow over the Gangetic Plains, weakening the climatological monsoon circulation (and moisture transports) over eastern India.

2.3. *Eurasia and Tibetan Plateau*

Springtime snow cover and snow depth over Eurasia and the Tibetan Plateau are also known to influence the South Asian (Bamzai and Shukla, 1999) and East Asian (Liu and Yanai, 2002b; Zhang *et al.*, 2004) summer monsoons. For example, increase in the spring snow depth over the Plateau since the late 1970s was linked with the westward expansion of the WPSH, and in turn to increased summer rainfall over the Yangtze River basin. As westward expansion of the WPSH was attributed to the Indian Ocean and Western Pacific warming from modeling studies (Zhou *et al.*, 2009b), the SST-warming in these basins has been suggested as a cause of the spring snow depth increase over Tibet (Zhang *et al.*, 2004). The weakened heating of the Tibetan Plateau contributes to weakening

of the East Asian summer monsoon circulation by reducing ocean-continent thermal contrast (Ding *et al.*, 2007; Duan and Wu, 2008).

2.4. *Low-frequency climate variability*

The climate system, including the Asian monsoon, exhibits multidecadal variability. Wang *et al.* (1981) and Zhu and Wang (2002) analyses of observed and reconstructed summer rainfall reveal the existence of an approximately 80-year variability timescale. Ding *et al.* (2007) have argued that the rainfall decline over northeastern China in the second half of the 20th century is a reflection of this intrinsic multidecadal variability. This idea has some support from the diagnostic analysis of Lei *et al.* (2011) who find natural decadal variability to be generally dominant. However, the increasing intensity of rainfall throughout China and the decrease in light rainfall days, particularly in the north, is, at least, partially of anthropogenic origin according to their analysis. The Atlantic Multidecadal Oscillation may also contribute to the multidecadal variability of the East Asian monsoon (Lu *et al.*, 2006).

3. Simulation of Monsoon Rainfall Trends by Climate System Models

The declining rainfall over the Gangetic Plain and the SFND trend over eastern China results from multiple influences, including anthropogenic ones. The relative contribution of these influences can be best assessed from experiments with the climate system models provided the modeled 20th century climate (forced by time-dependent greenhouse gas concentrations, aerosols and dust loadings, volcano injections, land-use land-cover, etc.) realistically captures the above-described subcontinental-scale, multidecadal monsoon precipitation trends.

The IPCC-AR5 models, unfortunately, do not rise to this challenge even via their ensemble-means. As shown in Fig. 4, only the GFDL-CM3 model captures the drying of the Gangetic Plain but it is unable to generate the SFND trend over eastern China. In fact, this model produces severe drying over the South-Flood region! There is a weak hint of the SFND trend in the ECHAM6-MPI simulation, which

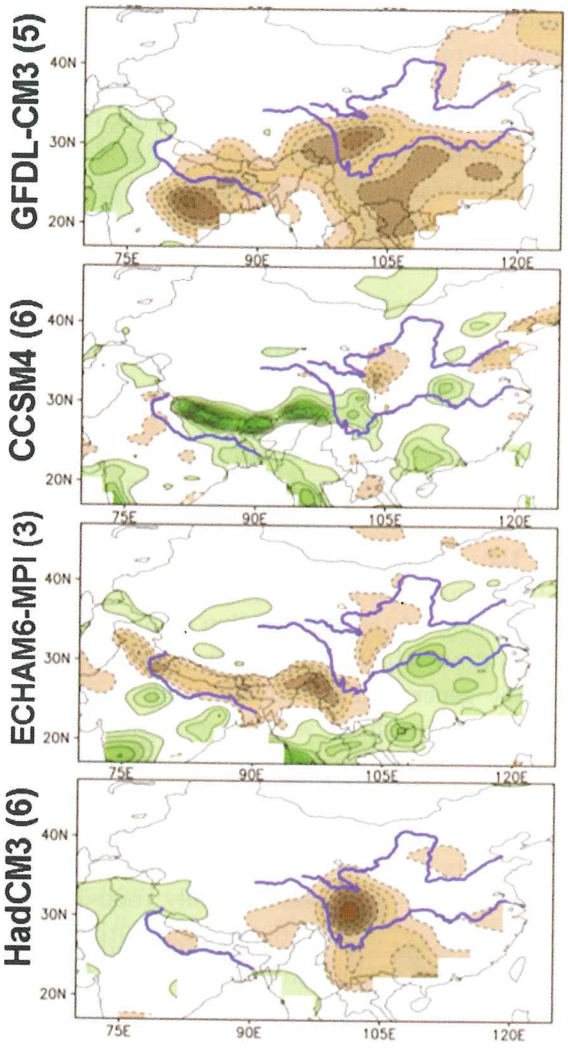

Fig. 4. The 1951–1999 linear trend in summer precipitation in the ensemble-mean CMIP5 simulations of 20th century climate by four leading IPCC-AR5 models. The number of ensemble members averaged in producing the ensemble-mean is indicated in brackets next to the model name. The trend is plotted at 0.5 mm/day/century interval, with deficit/surplus shown in brown/green, and the zero-contour omitted.

also contains elements of the Gangetic Plain rainfall trends. The climate system models limited skill in simulating the long-term trends in monsoon circulation and rainfall stems, in part, from their inability to generate realistic modes of multidecadal SST variability and/or related circulation and hydroclimate teleconnections to the continents.

4. Observationally Rooted Attribution of Monsoon Rainfall Trends

Climate system models are rapidly improving but evidently not ready for providing insights into the origin of regional hydroclimate trends. In the interim, analysis of the 20th century observations can perhaps provide a preliminary assessment of the contribution of multidecadal natural variability and anthropogenic change in the generation of rainfall trends over Asia. Such an assessment would necessarily have to be based on a climate system component with large thermal inertia (*e.g.*, ocean heat-content, or, perhaps, even just SST) so that multidecadal variability and secular change components can be unraveled. An observationally rooted analysis strategy is, of course, not without its own caveats, including the assumption of non-interaction (and thus separability) of the non-stationary secular trend and natural variability components.

4.1. *Spatiotemporal SST analysis*

Pacific and Atlantic SSTs were analyzed to obtain refined evolution descriptions from contextual separation of natural variability and the secular trend without advance filtering (and potential aliasing) of the SST record. The extended-EOF analysis technique (EEOF, Weare and Nasstrom, 1982) yields robust characterization of all non-seasonal modes of SST variability, including secular trend, from a single analysis of unfiltered data (Guan and Nigam, 2008). Mode physicality was assessed via correlations with the Pacific fish recruitment records, following Hare and Mantua (2000). The correlations were found comparable, if not larger, than those obtained by these authors; analog counts were also used in assessing mode physicality (Guan and Nigam, 2008). Atlantic SSTs were similarly analyzed but after removing the influence of Pacific SST variability and the SST Secular Trend from the Atlantic SST anomalies, leading, among others, to a clarified structure of Atlantic Multidecadal Oscillation (AMO; Guan and Nigam, 2009).

The Pacific SST principal components are shown in Fig. 5. By focusing on spatial and temporal recurrence but without imposition of periodicity constraints, EEOF analysis discriminates between biennial, El Nino Southern Oscillation (ENSO), and multidecadal variabilities in the Pacific: Canonical ENSO variability is captured as two modes: growth (ENSO) and decay (ENSO+). Deviation from canonical development, especially in the 1976/77-onward period is identified as a distinct mode, the ENSO non-canonical mode (ENSONC). Pacific decadal variability is resolved into two modes, Pan Pacific (PDVPP) and North Pacific (PDVNP). The former exhibits connections to the tropical-subtropical Atlantic resembling some AMO features. The latter captures the 1976/77 climate-shift, and is very close to Pacific Decadal Oscillation (PDO, Mantua *et al.*, 1997) in structure but with interesting links to the North Atlantic as well as the western tropical Pacific and Indian Ocean (Guan and Nigam, 2008). The nonstationary secular trend (SST-Trend) consists of widespread but non-uniform warming of all basins along with a sliver of cooling in the central equatorial Pacific.

4.2. *Rainfall reconstruction*

Reconstruction is based on the linear, summer regressions of the 11 SST PCs (7 Pacific and 4 Atlantic) on contemporaneous rainfall; the

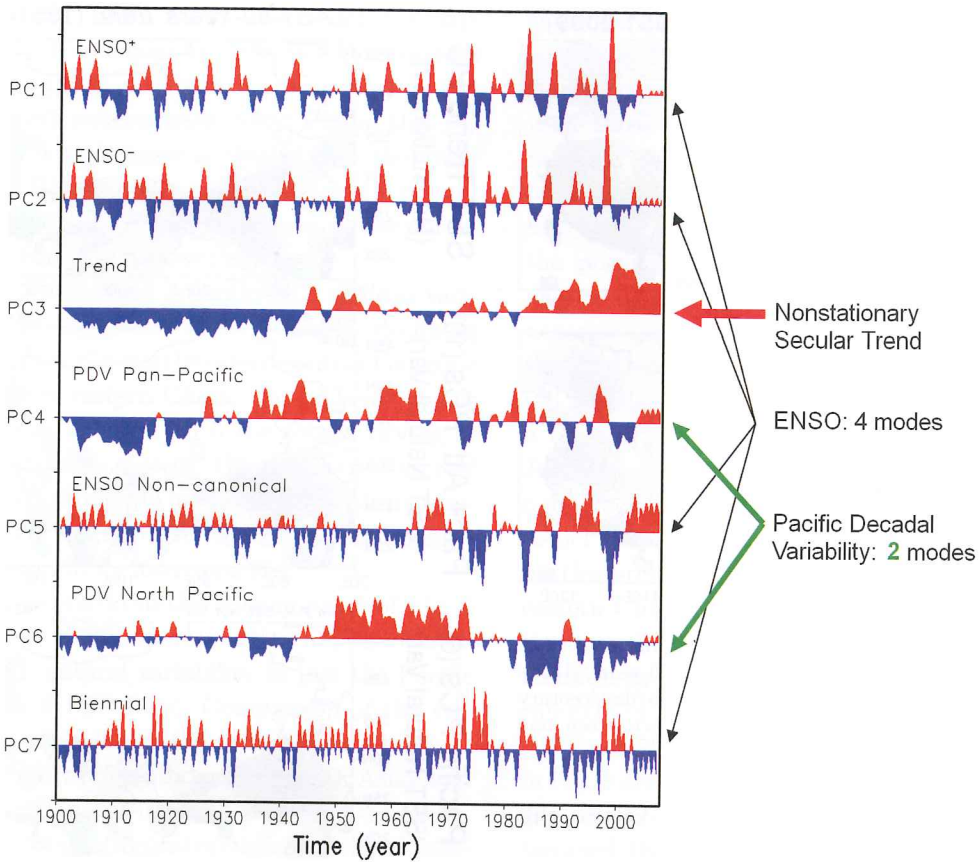

Fig. 5. SST principal components (PCs) from the extended-EOF (EEOF) analysis of HadISST 1.1 data. Seasonal anomalies during January 1900 — August 2009 were analyzed in the Pacific basin (20S-60N, 120E-60W) using 5-season-long anomaly sequences. The 7-leading PCs were rotated using the VARIMAX method. The EEOF technique is equivalent to multichannel singular spectrum analysis. See Guan and Nigam (2008, 2009) for more details.

regression period is summer 1901 to summer 2009, consistent with the CRU TS3.1 data span. The intra-basin PCs are temporally orthogonal (assured by the analysis method) while the inter-basin ones are nearly so (ensured by the filtering of Pacific's influence from Atlantic SSTs prior to their analysis; largest inter-basin PC correlation is 0.08), facilitating reconstruction of the rainfall anomalies. Multiplication of each SST PC (time varying) with its summer rainfall regression pattern (time invariant), and summing the 11 contributions yields the summer rainfall anomalies in this reconstruction. A similar strategy was recently used to reconstruct tropical cyclone counts in the Atlantic (Nigam and Guan, 2011) and precipitation variations (droughts) over the Great Plains (Nigam *et al.*, 2011).

The linear trend in the observed and reconstructed summer rainfall in the post-1950 period is compared in Fig. 6. The key trend features, including declining rainfall over the Gangetic Plain and the SFND pattern over eastern China, are robustly manifest in the reconstruction. Rainfall trends in the region south of the Yangtze River and further south over Indo-China are however somewhat weaker in the reconstruction.

Is the notable reconstruction of rainfall trends a result of over-fitting data with 11 SST

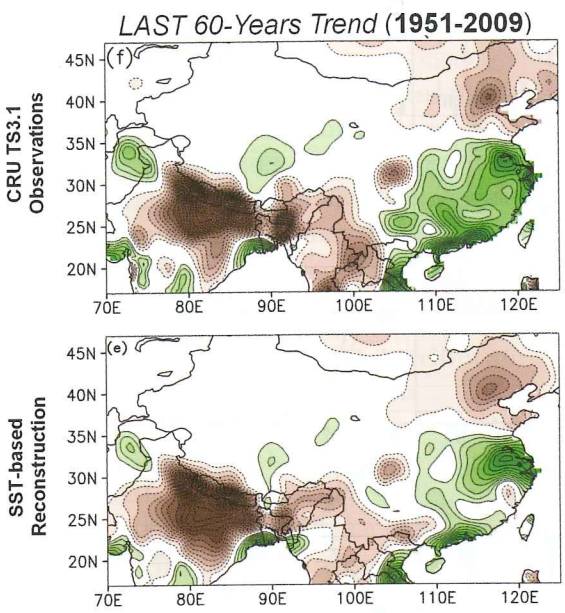

Fig. 6. The observed and reconstructed linear trend in summer monsoon rainfall over the last 60 years (1950–2009). The trend is plotted at 0.375 mm/day/century interval, with deficit/surplus shown in brown/green, and the zero-contour omitted.

PCs, or are just a few SST PCs key to this reconstruction?

4.3. *Analysis of reconstructed rainfall trend*

The reconstructed rainfall trend in the post-1950 period is parsed into 4 components in Fig. 7: The SST Secular Trend contribution is shown in the top panel while that of the remaining 10 SST PCs (referred together as Pacific and Atlantic SST natural variability) is in the second-from-top panel. The characterization of AMO as natural variability (*e.g.*, as above) has been challenged (Booth *et al.*, 2012) but this issue is moot in context of the present analysis in view of AMOs negligible contribution in the reconstruction of multidecadal precipitation trends (as shown next).

Comparison of the two indicates the considerable influence of both components. The

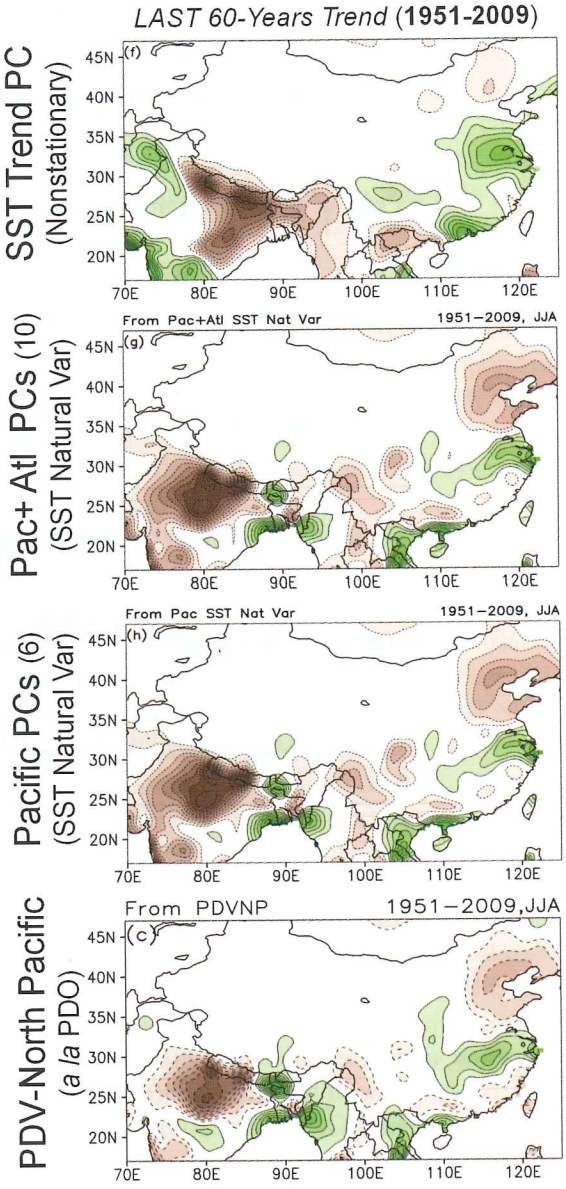

Fig. 7. Analysis of the reconstructed summer rainfall trend shown in Fig. 6 (bottom panel). The contribution of the SST Secular Trend is shown in the upper panel while that of SST natural variability in the Pacific and Atlantic basins in the second-from-top panel. Contribution of just Pacific SST natural variability is shown in the second-from-bottom panel. The trend contribution of just North Pacific decadal SST variability is shown in the bottom panel. The trend is plotted at 0.375 mm/day/century interval, with deficit/surplus shown in brown/green, and the zero-contour omitted.

SST Secular Trend PC is linked with the drying of the Himalayan foothills and northeastern Gangetic Plain, and with increasing rainfall in the western subcontinent. Over China, this PC is linked with increasing rainfall over the lower Yangtze River basin, i.e., over the southern center of the SFND dipole. Its influence over northeastern China is however modest.

The Pacific and Atlantic SST natural variability is associated with strongly declining rainfall over the northwestern-central Gangetic Plain. Over eastern China, this SST variability component is linked with the robust drying of the northeast, i.e., with the northern center of the SFND dipole. It is also linked with increasing rainfall but only over the immediate Yangtze River basin in its lower reaches.

The second-from-the-bottom panel of Fig. 7 shows the monsoon rainfall trends associated with SST natural variability in just the Pacific basin (or 6 SST PCs). Comparison of the two middle panels shows Atlantic SST variability to be minimally influential on the South Asian and East Asian summer-monsoon rainfall trends.

The notable reconstruction of summer rainfall trends (Fig. 6) thus results from contemporaneous regressions of just 7 SST PCs (SST Secular Trend and 6 Pacific PCs). Further analysis of the Pacific contribution (Fig. 7, bottom panel) shows that it results almost entirely from the influence of North Pacific decadal variability, referred as PDV-North Pacific or just PDV-NP in Guan and Nigam (2008) and in the figures here; its PC closely tracks the PDO index, as noted earlier. The post-1950 rainfall trends over monsoon Asia can thus be reconstructed from just 2 SST PCs, obviating any concerns regarding over-fitting of data.

5. North Pacific Decadal SST Variability and Asian Summer Monsoon Rainfall Trends

In view of the singular importance of North Pacific decadal SST variability (PDV-NP) for the summer monsoon rainfall trends over South Asia and East Asia (cf. Fig. 7), its SST and rainfall signatures are shown in Fig. 8, along with those of the PDO index. It is noteworthy that these were obtained from regressions on summer (JJA-averaged) anomalies over the full century (1901–2009 period), and not just the post-1950 period over which trends were analyzed. The PDV-NP links are shown for its negative phase to facilitate comparison with the PDO ones and the earlier displayed rainfall trends. A cooler midlatitude Pacific, with a band of cold SSTs extending eastward from Japan (until 140°W), characterizes the SST signal. The contemporaneous precipitation links depict the unmistakable rainfall deficit over the northwestern-central Gangetic Plain and northeastern China. An excessive rainfall signal over the immediate lower Yangtze River basin is also manifest in the PDV-NP regressions but not as robustly in the PDO ones.

The SST and precipitation anomalies shown in Fig. 8 are contemporaneous, leaving the cause and effect question open. Even if SSTs were assumed the cause, elaboration on the mechanism by which midlatitude Pacific SST anomalies impact rainfall over monsoon Asia would be challenging, as SST anomalies in only the Tropics are generally considered causative. Interestingly, the PDV-North Pacific is not without tropical links, notwithstanding its name. Guan and Nigam (2008) showed PDV-NP linked with the tropical Indian and Pacific basins; see also Deser *et al.* (2004). Figure 12 of Guan and Nigam shows SST regressions and correlations of the PDV-NP SST principal component. The correlation map readily reveals the tropical links, especially in the Indian Ocean and Western Pacific where smaller amplitudes of SST variability create a detection challenge, but not for the correlation statistic.

The tropical SST links of PDV-NP are, moreover, shown to be of opposite sign to the midlatitude ones (Guan and Nigam, 2008; Fig. 12). Declining summer rainfall over the

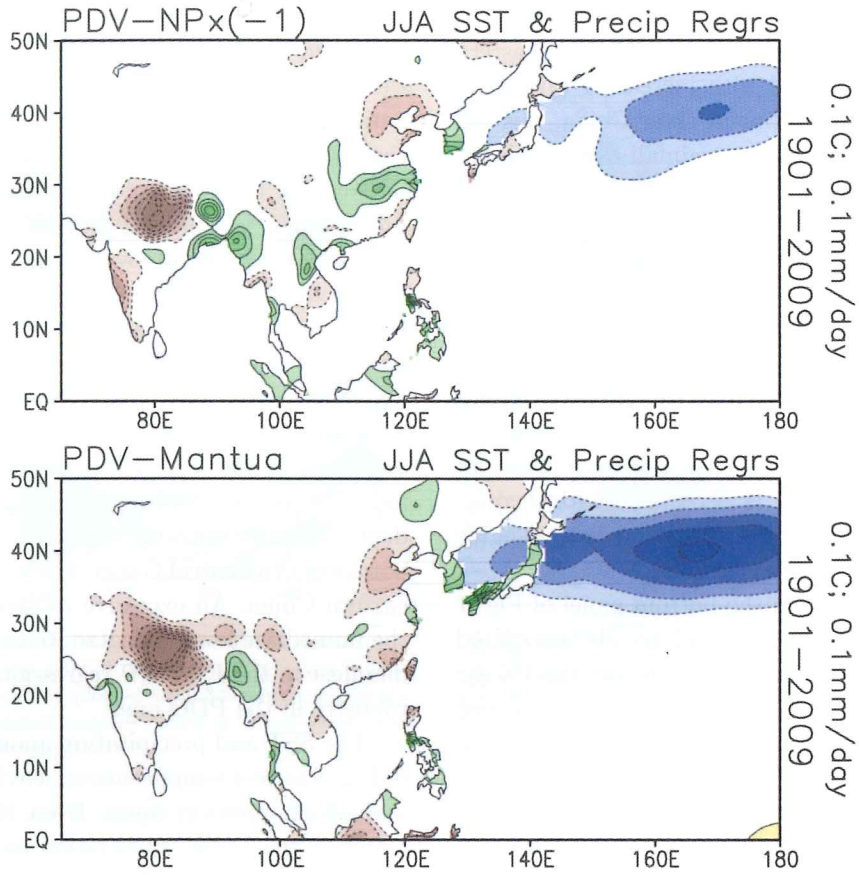

Fig. 8. The summer (JJA) precipitation and SST regressions of Pacific Decadal Variability (PDV) for the 1901–2009 period. The top panel shows regressions of the PDV-North Pacific principal component (for the opposite phase shown in Fig. 5), while the lower panels shows the same for the Pacific Decadal Oscillation (PDO) index, a commonly used marker for decadal SST variability in the North Pacific. The SST regressions are contoured with 0.1K interval, with cold/warm anomalies shown in blue/red. Precipitation regressions are contoured with a 0.1 mm/day interval, with deficits/surplus shown in brown/green. The zero-contour is omitted, as before.

northwestern-central Gangetic Plain and northeastern China is thus also linked with a warmer Indo-Pacific basin to the immediate south of the Asian Continent. Although the mechanisms by which the multi-basin SST footprint of PDV-NP influences regional summer rainfall over the Asian Continent remains to be elucidated, at least the sign of the SST anomalies in the tropical Indian and Western Pacific basins is consistent with the basic understanding of the monsoon mechanism — that large-scale land-ocean thermal contrast is the driver. Anomalously warm SSTs to the south of the Asian landmass would weaken the summertime contrast, leading to large-scale reduction in monsoon rainfall. The observed summer rainfall trends however exhibit complex spatial structure, reflecting the significance of regional interactions rooted in heterogeneous terrain and coastlines, and massive orographic complexes, including Tibetan Plateau. Clearly, an investigation of the origin of the post-1950 summer rainfall trends over the Asian Continent will require controlled modeling experiments with a climate system model that can generate realistic patterns of seasonal, interannual,

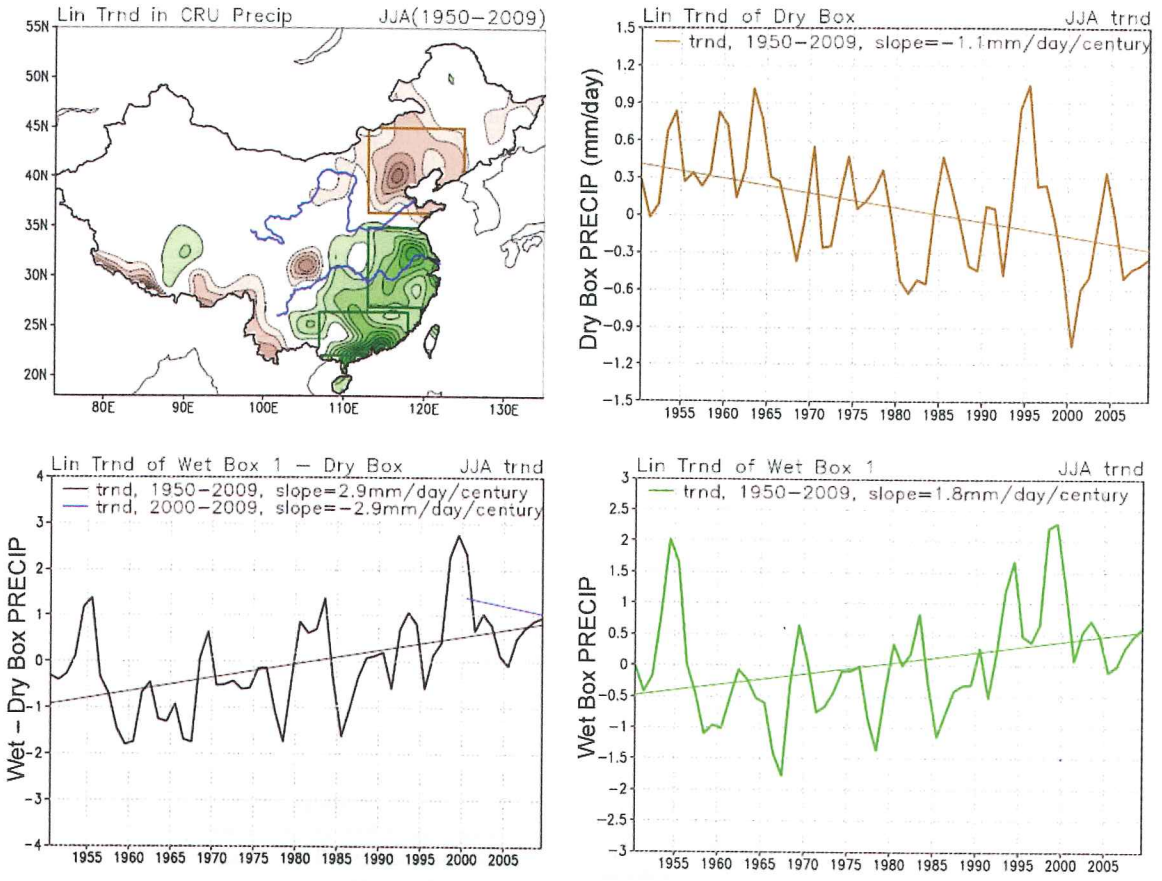

Fig. 9. Area-averaged summer (JJA) precipitation anomaly with respect to the 1901–2009 mean in the North-Drought (Dry Box, top-right panel) and South-Flood (Wet Box 1, bottom-right) core region of the SFND trend pattern. The boxed regions are marked with brown and green lines in the top-left panel which shows the 1950–2009 period linear trend in summer rainfall at intervals of 0.5 mm/day/century; Wet Box 1 refers to the box encompassing the lower Yangtze River. The Wet Box 1 minus Dry Box precipitation anomaly a marker of the strength of the SFND pattern is plotted in the bottom-left panel. All precipitation anomalies are plotted in mm/day units, and the post-1950 period linear trend is plotted in each panel with the slope noted. The recent 10-year (2000–2009) slope is also shown in the bottom-left panel as its negative sign has prompted some to suggest that the SFND pattern is weakening; however such short-period weakening is not uncommon in the considered period (*e.g.*, 1955–1965).

and decadal/multidecadal variability in regional rainfall — a challenging target for the current model class (IPCC-AR5), as shown in Fig. 4.

6. Concluding Remarks

Analysis of the century-long precipitation and SST records suggests that the recent (post-1950) decline in rainfall over the northwestern-central Gangetic Plain and northeastern China is linked with North Pacific decadal SST variability (closely related to the PDO). The rainfall decline over the Himalayan foothills and northeastern Gangetic Plain, and increasing rainfall over the lower Yangtze River basin (the southern SFND center), on the other hand, are found linked with SST Secular Trend (or secular variability).

An elucidation of the mechanisms generating the indicated links would require elaborate

observational analyses keyed to lead-lag regressions on 3D thermodynamic and circulation fields, many of which are unfortunately unavailable for a significant portion of the 20th century. The SST links of the declining summer rainfall over the Gangetic Plain are however broadly consistent with the rudimentary monsoon mechanism, imparting some dynamical support for the observational findings. Controlled experiments with climate system models that replicate Asian precipitation and circulation climatology, interannual variability, and multidecadal trends can be potentially insightful but such models are presently unavailable, as noted earlier.

This investigation of the role of decadal SST variability in generation of multidecadal rainfall trends was instigated by the findings of both increasing and decreasing trends over the Gangetic Plain; the former in the first-half of the 20th century. The analysis of increasing trends in the first half-century is not reported for reasons of space, but reconstruction of rainfall trends in this period suggests a significant role of the Pan-Pacific mode of decadal SST variability (PDV-PP; see Fig. 11 and related discussion in Guan and Nigam, 2008). The PDV-PP has robust footprints also in the western Atlantic resembling AMOs tropical structure; the AMO and PDV-PP are correlated at $\sim$0.45.

Finally, inspection of the rainfall record has led some to conclude that the SFND trend pattern has weakened recently. The area-averaged rainfall anomaly over the SFND core regions is plotted in Fig. 9, separately for the North-Drought and South-Flood sectors to investigate this issue. The right panels in Fig. 9 do not show any notable modulation of the decreasing and increasing rainfall trends; nor is trend modulation apparent in the wet-minus-dry index (bottom-left panel). To be sure, this index exhibits decadal fluctuations, including periods of abatement but not just in the recent decade; for example, note the index decline during 1955–1965.

The present analysis is focused on the half-century-long trends; not decadal ones which could easily result from the interference of interannual and decadal variabilities.

References

Bamzai, A., and J. Shukla, 1999: Relation between Eurasian Snow Cover, Snow Depth, and the Indian Summer Monsoon: An Observational Study. *J. Climate*, **12**, 3117–3132.

Bollasina, M. A., Y. Ming, and V. Ramaswamy, 2011: Anthropogenic aerosols and the weakening of the South Asian summer monsoon. *Science*, **334**, 502–505 (28 October 2011).

———, and S. Nigam, 2011: Modeling of Regional Hydroclimate Change over the Indian Subcontinent: Impact of the Expanding Thar Desert. *J. Climate*, **24**, 3089–3106.

Booth, B. B. B., N. J. Dunstone, P. R. Halloran, T. Andrews, and N. Bellouin, 2012: Aerosols implicated as a prime driver of twentieth-century North Atlantic climate variability. *Nature*, **484**, 228–232 (12 April 2012).

Deser, C., A. S. Phillips, and J. W. Hurrell, 2004: Pacific Interdecadal Climate Variability: Linkages between the Tropics and the North Pacific during Boreal Winter since 1900. *J. Climate*, **19**, 3109–3124.

Ding, Y. H., Z. Wang, and Y. Sun, 2007: Inter-decadal variation of the summer precipitation in East China and its association with decreasing Asian summer monsoon. Part I: Observed evidences. *Int. J. Climatol.*, **28**, 1139–1161, doi:10.1002/joc.1615.

Duan, A. M., and G. X. Wu, 2008: Weakening Trend in the Atmospheric Heat Source over the Tibetan Plateau during Recent Decades. Part I: Observations. *J. Climate*, **21**, 3149–3164.

Guan, B., and S. Nigam, 2008: Pacific Sea Surface Temperatures in the Twentieth Century: An evolution-centric analysis of variability and trend. *J. Climate*, **21**, 2790–2809.

———, 2009: Analysis of Atlantic SST variability factoring inter-basin links and the secular trend: Clarified structure of the Atlantic Multidecadal Oscillation. *J. Climate*, **22**, 4228–4240.

Hare, S. R., and N. J. Mantua, 2000: Empirical evidence for North Pacific regime shifts in 1977 and 1989. *Prog. Oceanogr.*, **47**, 103–145.

Lau, K.-M., and K.-M. Kim, 2006: Observational relationships between aerosol and Asian monsoon rainfall, and circulation, *Geophys. Res. Lett.*, **33**, L21810, doi:10.1029/2006GL027546.

Lei, Y., B. Hoskins, and J. Slingo, 2011: Exploring the interplay between natural decadal variability and anthropogenic climate change in summer rainfall over China. Part I: Observational evidence. *J. Climate*, **24**, 4584–4599.

Li, H., A. Dai, T. Zhou, and J. Lu, 2010: Responses of East Asian summer monsoon to historical SST and atmospheric forcing during 1950–2000. *Climate Dyn.*, **34**, 501–514.

Liu, X. D., and M. Yanai, 2002: Influence of Eurasian spring snow cover on Asian summer monsoon rainfall. *Int. J. Climatol.*, **25**, 1075–1089.

Lu, R., B. Dong, and H. Ding, 2006: Impact of the Atlantic Multidecadal Oscillation on the Asian summer monsoon. *Geophys. Res. Lett.*, **33**, L24701, doi:10.1029/2006GL027655.

Mantua, N. J., S. R. Hare, Y. Zhang, J. M. Wallace, and R. C. Francis, 1997: A Pacific interdecadal climate oscillation with impacts on salmon production. *Bull. Amer. Meteor. Soc.*, **78**, 1069–1079.

Meehl, G. A., J. M. Arblaster, and W. D. Collins, 2008: Effects of black carbon aerosols on the Indian monsoon, *J. Climate*, **21**, 2869–2882.

Menon, S., J. Hansen, L. Nazarenko, and Y. Luo, 2002: Climate effects of black carbon aerosols in China and India, *Science*, **297**, 2250–2253.

Mitchell T. D., and P. D. Jones, 2005: An improved method of constructing a database of monthly climate observations and associated high-resolution grids. *Int. J. Climatol.*, **25**, 693–712.

Nigam, S., B. Guan, and A. Ruiz-Barradas, 2011: Key role of the Atlantic Multidecadal Oscillation in 20th century drought and wet periods over the Great Plains. *Geophys. Res. Lett.*, **38**, L16713, doi:10.1029/2011GL048650.

———, and B. Guan, 2011: Atlantic Tropical Cyclones in the 20th Century: Natural Variability and Secular Change in Cyclone Count. *Climate Dynamics*, **36**, 2279–2293, doi: 10.1007/s00382-010-0908-x.

Piao, S., *et al.*, 2010: The impacts of climate change on water resources and agriculture in China. *Nature*, **467**, 43–51.

Ramanathan, V., and Coauthors, 2005: Atmospheric Brown Clouds: Impacts on South Asian Climate and Hydrological Cycle. *PNAS*, **102**, 5326–5333.

Schneider, U., T. Fuchs, A. Meyer-Christoffer, and B. Rudolf, 2008: Global precipitation analysis products of the GPCC. Global Precipitation Climatology Centre (GPCC), DWD, *Internet Publication*, 1–12.

Wang, S. W., Z. Zhao, and Z. Chen, 1981: Reconstruction of the summer rainfall regime for the last 500 years in China. *Geophys. J.*, **52**, 117–122.

Weare, B. C., and J. S. Nasstrom, 1982: Examples of extended empirical orthogonal function analyses. *Mon. Wea. Rev.*, **110**, 481–485.

Willmott, C. J., and K. Matsuura, 1995: Smart Interpolation of Annually Averaged Air Temperature in the United States. *J. Appl. Meteorol.*, **34**, 2577–2586.

Yatagai, O. Arakawa, K. Kamiguchi, H. Kawamoto, M. I. Nodzu, and A. Hamada, 2009: A 44-year daily precipitation dataset for Asia based on dense network of rain gauges. *SOLA*, **5**, 137–140, doi:10.2151/sola.2009-035.

Yu, R. C., and T. J. Zhou, 2007: Seasonality and three-dimensional structure of the interdecadal change in East Asian monsoon, *J. Climate*, **20**, 5344–5355.

Zhang, Y. S., T. Li, and B. Wang, 2004: Decadal change of the spring snow depth over the Tibetan Plateau: The associated circulation and influence on the East Asian summer monsoon. *J. Climate*, **17**, 2780–2793.

Zhou, T., D. Gong, J. Li, and B. Li, 2009a: Detecting and understanding the multidecadal variability of the East Asian summer monsoon — Recent progress and state of affairs. *Meteor.Zeitschrift*, **18**, 4, 455–467.

———, R. Yu, J. Zhang, H. Drange, C. Cassou, C. Deser, D. L. R. Hodson, E. Sanchez-Gomez, J. Li, N. Keenlyside, X. Xin, and Y. Okumura, 2009b: Why the western pacific subtropical high has extended westward since the late 1970s. *J. Climate*, **22**, 2199–2215.

Zhu, J., and S. Wang, 2002: 80 yr oscillation of summer rainfall over North China and East Asian Summer Monsoon. *Geophys. Res. Lett.*, **14**, 1672, doi:10.1029/2001GL013997.